Published in final edited form as:
Neuroscience. 2009 February 18; 158(4): 1577–1588. doi:10.1016/j.neuroscience.2008.11.039.

Signaling Mechanisms Mediating Muscarinic Enhancement of GABAergic Synaptic Transmission in the Spinal Cord

Hong-Mei Zhang[1], **Shao-Rui Chen**[1], **You-Qing Cai**[1], **Timothy E. Richardson**[1], **Larry C. Driver**[1], **Gabriel Lopez-Berestein**[2], and **Hui-Lin Pan**[1,3]

1*Department of Anesthesiology and Pain Medicine, The University of Texas M. D. Anderson Cancer Center Houston, TX 77030*

2*Department of Experimental Therapeutics, The University of Texas M. D. Anderson Cancer Center Houston, TX 77030*

3*Program in Neuroscience, The University of Texas Graduate School of Biomedical Sciences Houston, TX 77225*

Abstract

Activation of muscarinic acetylcholine receptors (mAChRs) inhibits spinal nociceptive transmission by potentiation of GABAergic tone through M_2, M_3, and M_4 subtypes. To study the signaling mechanisms involved in this unique mAChR action, GABAergic spontaneous inhibitory postsynaptic currents (sIPSCs) of lamina II neurons were recorded using whole-cell patch clamp techniques in rat spinal cord slices. The mAChR agonist oxotremorine-M caused a profound increase in the frequency of GABAergic sIPSCs, which was abolished in the Ca^{2+}-free solution. Inhibition of voltage-gated Ca^{2+} channels with Cd^{2+} and Ni^{2+} largely reduced the effect of oxotremorine-M on sIPSCs. Blocking nonselective cation channels (NSCCs) with SKF96365 or 2-APB also largely attenuated the effect of oxotremorine-M. However, the KCNQ channel blocker XE991 and the adenylyl cyclase inhibitor MDL12330A had no significant effect on oxotremorine-M-induced increases in sIPSCs. Furthermore, the phosphoinositide-3-kinase (PI3K) inhibitor wortmannin or LY294002 significantly reduced the potentiating effect of oxotremorine-M on sIPSCs. In the spinal cord in which the M_3 subtype was specifically knocked down by intrathecal siRNA treatment, SKF96365 and wortmannin still significantly attenuated the effect of oxotremorine-M. In contrast, SKF96365 and wortmannin both failed to alter the effect of oxotremorine-M on sIPSC when the M_2/M_4 mAChRs were blocked. Therefore, our study provides new evidence that activation of mAChRs increases synaptic GABA release through Ca^{2+} influx and voltage-gated Ca^{2+} channels. The PI3K-NSCC signaling cascade is primarily involved in the excitation of GABAergic interneurons by the M_2/M_4 mAChRs in the spinal dorsal horn.

Introduction

The cholinergic system and muscarinic acetylcholine receptors (mAChRs) have an important function in the regulation of pain transmission at the spinal cord level. For example, blocking

Address correspondence to Hui-Lin Pan, M.D., Ph.D., Department of Anesthesiology and Pain Medicine, Unit 110, The University of Texas M. D. Anderson Cancer Center, 1515 Holcombe Blvd., Houston, TX 77030. Tel: (713) 563-5838; Fax: (713) 794-4950; E-mail: huilinpan@mdanderson.org.

spinal mAChRs with atropine causes a large increase in pain sensitivity (Zhuo and Gebhart, 1991). Also, intrathecal administration of mAChR agonists or acetylcholinesterase inhibitors produces potent analgesia in rodents and in humans (Iwamoto and Marion, 1993, Hood et al., 1997, Duttaroy et al., 2002, Li et al., 2002). Molecular cloning studies have revealed five molecularly distinct mAChRs referred to as M_1-M_5 (Caulfield et al., 1994, Wess, 2003). The odd-numbered subtypes are selectively linked to $G_{q/11}$ proteins to activate phospholipase C, while the even-numbered subtypes are classically coupled to the pertussis toxin-sensitive $G_{i/o}$ proteins (Caulfield and Birdsall, 1998, Wess, 2003). Previous studies have shown that M_2, M_3, and M_4 mAChRs are present in the spinal dorsal horn (Hoglund and Baghdoyan, 1997, Yung and Lo, 1997, Li et al., 2002, Chen et al., 2005). The highest density of mAChRs in the spinal cord is present in the superficial lamina in both rats and humans (Yamamura et al., 1983, Scatton et al., 1984, Villiger and Faull, 1985, Li et al., 2002). Using mAChR subtype-knockout mice, it has been demonstrated that the M_2 and M_4 are the most important subtypes for the analgesic effects of mAChR agonists (Duttaroy et al., 2002, Wess, 2003). However, little is known about the cellular and signaling mechanisms involved in this mAChR action in the spinal cord.

At the spinal level, one of the key mechanisms by which mAChR activation inhibits nociceptive transmission is through potentiation of synaptic GABA release (Baba et al., 1998, Zhang et al., 2005). Increased GABAergic synaptic transmission can reduce the nociceptive input from primary afferents through presynaptic $GABA_B$ receptors (Li et al., 2002, Chen and Pan, 2004). We showed previously that M_2, M_3, and M_4 mAChRs are all involved in the stimulation of GABAergic interneurons in the rat spinal cord (Zhang et al., 2005). It is well known that the M_3 subtype is selectively linked to $G_{q/11}$ proteins and produces its stimulating effect through phospholipase C–ionsitol-1,4,5-triphosphate/diacylglycerol–protein kinase C and intracellular Ca^{2+} release (May et al., 1999, Evellin et al., 2002). However, the downstream signaling mechanisms leading to the increased excitability of GABAergic neurons by M_2 and M_4 subtypes in the spinal cord remain poorly understood. The potentiating effect of mAChR agonists on GABAergic interneurons is especially puzzling, because both M_2 and M_4 subtypes are typically coupled to the inhibitory $G_{i/o}$ proteins. Therefore, in the present study, we explored signal transduction mechanisms underlying the distinct enhancement of GABAergic synaptic transmission by mAChR activation in the spinal dorsal horn.

Methods

Male Sprague-Dawley rats (6-8 weeks old; Harlan, Indianapolis, IN) were used in this study. All the surgical and experimental protocols were approved by the Animal Care and Use Committee of the University of Texas M. D. Anderson Cancer Center and conformed to the NIH guidelines on the ethical use of animals.

Spinal cord slice preparation

Rats were anesthetized with 2% isoflurane in O_2 and the lumbar segment of the spinal cord was rapidly removed through laminectomy. The rats then were killed by inhalation of 5% isoflurane. The lumbar segment was immediately placed in ice-cold sucrose artificial cerebrospinal fluid (aCSF) presaturated with 95% O_2 and 5% CO_2. The sucrose aCSF contained (mM) sucrose, 234; KCl, 3.6; $MgCl_2$, 1.2; $CaCl_2$, 2.5; NaH_2PO_4, 1.2; glucose, 12.0; and $NaHCO_3$, 25.0. The tissue was then placed in a shallow groove formed in a gelatin block and glued onto the stage of a vibratome (Technical Product International, St. Louis, MO). Transverse spinal cord slices (400 μm) were cut in the ice-cold sucrose aCSF and then preincubated in Krebs solution oxygenated with 95% O_2 and 5% CO_2 at 34°C for at least 1 h before they were transferred to the recording chamber. The Krebs solution contained (mM) NaCl, 117.0; KCl, 3.6; $MgCl_2$, 1.2; $CaCl_2$, 2.5; NaH_2PO_4, 1.2; glucose, 11.0; and $NaHCO_3$,

25.0. Each slice was then placed in a glass-bottomed chamber (Warner Instruments, Hamden, CT) and fixed with parallel nylon threads supported by a U-shaped stainless steel weight. The slice was continuously perfused with Krebs solution at 5.0 ml/min at 34°C maintained by an inline solution heater and a temperature controller (TC-324; Warner Instruments).

Electrophysiological recordings

Recordings of postsynaptic currents were performed using the whole-cell voltage-clamp method, as we described previously (Zhang et al., 2005, Zhang et al., 2006a). The lamina II has a distinct translucent appearance and can easily be distinguished under the microscope. The neurons located in the lamina II of the spinal slices were identified under a fixed stage microscope (BX50WI, Olympus, Tokyo, Japan) with differential interference contrast/infrared illumination. The electrode for the whole-cell recordings was pulled from borosilicate glass capillaries with a puller (P-97, Sutter Instrument, Novato, CA). The impedance of the pipette was 4-7 MΩ when filled with internal solution containing (mM) Cs_2SO_4, 110; KCl, 5; $MgCl_2$, 2.0; $CaCl_2$, 0.5; HEPES, 5.0; EGTA, 5.0; ATP-Mg, 5.0; Na-GTP, 0.5; guanosine 5'-*O*-(2-thiodiphosphate) (GDP-β-S), 1; and QX314, 10. Recordings of postsynaptic currents began 5-7 min after whole-cell access was established and the current reached a steady state. The input resistance was monitored and the recording was abandoned if it changed by more than 15%. Signals were recorded using an amplifier (MultiClamp 700A, Axon Instruments, Foster City, CA) at a holding potential of 0 mV, filtered at 1-2 kHz, digitized at 10 kHz, and stored in a computer. All GABAergic spontaneous inhibitory postsynaptic currents (sIPSCs) were recorded at a holding potential of 0 mV (Zhang et al., 2005) in the presence of 2 μM strychnine, a glycine receptor antagonist.

Formulation of chitosan-siRNA nanoparticles

A 21-bp sequence targeting the M_3 subtype, 5'-AAG'GAG'AGG'CAT'ACC'GCT'AAA-3' (2005-2025; Genebank Accession no: NM_012527), was selected as the M_3 siRNA using web-based design software. A 4-base mismatched sequence, 5'-AAG'G**C**G'AGG'C**T**T'ACC' G**G**T'AA**C**-3', was used as the control siRNA. We performed BLAST search (National Center for Biotechnology Information Database) to minimize the potential off-target effects of siRNA sequences. All chemically synthesized siRNA duplexes with more than 90% purity were obtained from Qiagen (Valencia, CA). It has been shown that an efficient way to deliver siRNA *in vivo* is by using chitosan-siRNA nanoparticles (Howard et al., 2006, Liu et al., 2007). In addition to its advantages such as biodegradability and biocompatibility, chitosan is an attractive vector for siRNA delivery because its protonated amine groups allow transport across cellular membranes and subsequent endocytosis into the neurons (Howard et al., 2006, Katas and Alpar, 2006, Liu et al., 2007). Furthermore, positively charged amines (under slightly acidic conditions) permit electrostatic interaction with phosphate-bearing nucleic acids to form polyelectrolyte complexes. Chitosan-siRNA nanoparticles were prepared as described previously (Katas and Alpar, 2006). Briefly, chitosan (Aldrich) was dissolved in 1% acetate buffer and was adjusted to pH 4.6 with 10 N NaOH. Sodium tripolyphosphate solution (0.25%, w/v) containing the siRNA (70 μg/ml) was added to the chitosan solution (5 mg/ml) with fast stirring. After 30 min, the mixture was centrifuged at 9,000 g for another 30 min at 4°C. The pellet was then diluted with sterile RNase-free water to obtain the final concentration of 1 μg/μl chitosan-siRNA solution.

Intrathecal treatment with siRNA

Intrathecal catheters were inserted into rats anesthetized using 2% isoflurane. The catheters (polyethylene-10 tubing) were inserted through an incision in the cisternal membrane and advanced so that the tip of each catheter was positioned at the lumbar spinal level. Rats were injected with intrathecal siRNA for three consecutive days with a dose of 5 μg each day. In the

pilot experiments, we observed that this treatment protocol resulted in the maximal knockdown of the mAChR subtypes in the spinal cord. The rats were used for the final electrophysiological experiments or quantitative RT-PCR analysis 3-4 days after the last siRNA injection.

RNA isolation and quantitative RT-PCR analysis

Three-four days after the last siRNA injection, animals were killed by inhalation of 5% isoflurane. The total RNA was extracted from the dorsal half of the lumbar spinal cord using Purelink RNA Purification System (Invitrogen, Carlsbad, CA) with on-column DNase I digestion according to the manufacturer's instructions. cDNA synthesis was performed by reverse transcription of each sample by using Superscript III first strand synthesis kit (Invitrogen). Real-time PCR was performed using the ABI Prism 7700 sequence detection system with SYBR green PCR core reagents kit (Applied Biosystems, Foster City, CA). All samples were run in duplicate using an annealing temperature of 60°C. The primer sets used (Invitrogen) are listed in Table 1. The amount of target mRNA in each reaction was determined from the detection threshold cycle number (Ct), which is inversely correlated with the abundance of the mRNA level. To calculate the relative amount of target mRNA, standard curves were generated by a 2-fold dilution of the spinal cord cDNA as the PCR templates. For each sample, the relative amount of the target mRNA was first normalized to β-actin mRNA and then normalized by setting the mRNA expression level of the control siRNA-treated animals as 1. The specificity of the PCR products was confirmed by the melting curve analysis and agarose gel electrophoresis.

Quantification of the M_3 membrane protein level using immunoprecipitation and radioactive binding

The following immunoprecipitation and radioligand binding experiments were performed to quantify the M_3 protein level in the spinal cord in M_3 siRNA- and control siRNA-treated rats. The lumbar spinal cords were quickly harvested from rats under 2-3% isoflurane. The spinal cord tissue was homogenized in ice-cold 0.32 M sucrose in 5 mM Tris-HCl buffer containing 1 mM phenylmethanesulfonyl fluoride. The homogenate was centrifuged at 500 g for 10 min at 4°C. The pellet was discarded, and the supernatant was centrifuged again at 48,000 g for 20 min at 4°C. Then the pellet was resuspended in assay buffer (25 mM phosphate buffer containing 5 mM $MgCl_2$ and 1 mM phenylmethanesulfonyl fluoride, pH 7.4) and was centrifuged as described above. The final pellet was resuspended in 3 ml of the same buffer and sonicated for 5 s. The membrane protein was subsequently incubated for 1 hr with 2 nM [^{3}H]quinuclidinyl benzilate ([^{3}H]QNB), the nonselective mAChR antagonist (42 Ci/mmol; PerkinElmer Life and Analytical Sciences), in the final volume of 1 ml. After washing thoroughly, the labeled membranes were solubilized with 1% digitonin and followed by immunoprecipitation of solubilized [^{3}H]QNB-labeled receptors with the M_3 subtype-selective antiserum, as we described previously (Chen et al., 2005). Radioactivity was quantified using a Beckman LS6500 scintillation counter. Binding data were processed using the GraphPad Prism program.

Chemicals

Oxotremorine-M, GDP-β-S, cadmium, nickel, MDL12330A, himbacine, and strychnine were obtained from Sigma-Aldrich. Mibefradil, XE991, and SKF96365 were purchased from Tocris (Ellisville, MO). Wortmannin and LY294002 were obtained from Alexis (San Diego, CA). QX314 and 2-APB were purchased from Alomone Labs (Jerusalem, Israel) and Cayman Chemical (Ann Arbor, MI), respectively. Drugs were dissolved in Krebs solution and perfused into the slice chamber using syringe pumps. The effective concentrations of the above drugs for bath application have been determined in previous studies using spinal or brain slices and tested in preliminary experiments.

Data analysis

Data are presented as means ± SEM. The sIPSCs were analyzed off-line with a peak detection program (MiniAnalysis, Synaptosoft, Leonia, NJ). Measurements of the amplitude and frequency of sIPSCs were performed over a period of at least 1 min during control, drug application, and recovery. For each analysis, 300-1500 events were included. The sIPSCs were detected by the fast rise time of the signal over an amplitude threshold (typically 5-6 pA) above the background noise. We manually excluded the event when the noise was erroneously identified as the sIPSCs by the program. In each of the neurons tested, the cumulative probability of the amplitude and the inter-event interval of sIPSCs were compared using the Kolmogorov-Smirnov test. This test was used first to determine whether the effect of oxotremorine-M on sIPSCs was significantly different in individual neurons. The drug effects on oxotremorine-M-induced increase in the frequency of sIPSCs and the effect of siRNA treatment on the expression levels of mRNA and proteins were determined by either paired two-tailed Student's *t*-test or repeated measures analysis of variance with Tukey's post hoc test. $P < 0.05$ was considered to be statistically significant.

RESULTS

Stimulation of mAChRs evokes GABA release through Ca^{2+} influx

To study the role of extracellular Ca^{2+} in oxotremorine-M-induced GABA release, we compared the effect of 3 μM oxotremorine-M on the frequency of GABAergic sIPSCs in Krebs and Ca^{2+}-free bath solutions. Initial bath application of 3 μM oxotremorine-M in Krebs solution for 3 min caused a large increase in the frequency of sIPSCs (ranging from 1.64 to 7.92 Hz, n = 8 neurons, Fig. 1, A-C). Similar to what we reported previously (Zhang et al., 2005), 3 μM oxotremorine-M also significantly increased the amplitude (from 12.43 to 24.43 pA) of sIPSCs in about 50% of neurons tested. Because the potentiating effect of oxotremorine-M on the amplitude and frequency of GABAergic sIPSCs is blocked by tetrodotoxin, mAChRs are likely located on the somatodendritic site of GABAergic interneurons in the spinal dorsal horn (Zhang et al., 2005). For the sake of simplicity, we focused our analysis mainly on the frequency of sIPSCs in the following protocols.

After washout of the initial effect of oxotremorine-M, the Ca^{2+}-free solution was perfused into the bath for 10 min. The basal frequency of sIPSCs was significantly reduced in the Ca^{2+}-free solution. Furthermore, repeat application of 3 μM oxotremorine-M failed to significantly change sIPSCs in the Ca^{2+}-free solution (n = 11 neurons, Fig. 1, A-C). When Krebs solution was re-introduced into the bath chamber, oxotremorine-M significantly increased the frequency of sIPSCs in the neurons (Fig. 1C). In another 11 neurons, repeated application of 3 μM oxotremorine-M for 3 min in the Krebs solution caused a similar increase in the frequency of sIPSCs (Fig. 1D). These results suggest that activation of spinal mAChRs stimulates synaptic GABA release and that this effect critically depends upon the presence of extracellular Ca^{2+}.

Synaptic GABA release by mAChR activation is mediated by voltage-gated Ca^{2+} channels

Because voltage-gated Ca^{2+} channels play a major role in Ca^{2+} influx during neuronal depolarization, we next determined the role of voltage-gated Ca^{2+} channels in oxotremorine-M-induced synaptic GABA release in the spinal cord. The high voltage-gated Ca^{2+} channel blocker Cd^{2+} (Bao et al., 1998, Wu et al., 2004) was used. Bath application of 100 μM $CdCl_2$ alone significantly decreased the baseline frequency of GABAergic sIPSCs in all of the neurons tested. The stimulating effect of 3 μM oxotremorine-M on the frequency of sIPSCs was largely blocked by Cd^{2+} (n = 14, Fig. 2, A-C).

Because low voltage-gated (T-type) Ca^{2+} channels also mediate neurotransmitter release in the spinal dorsal horn (Bao et al., 1998), we next used the selective T-type Ca^{2+} channel blocker

Ni^{2+} (100 μM) or mibefradil (100 μM). The potentiating effect of oxotremorine-M on sIPSCs was significantly reduced by mibefradil (n = 9, Fig. 2D) or Ni^{2+} (n = 7, Fig. 2E). Furthermore, the effect of oxotremorine-M on synaptic sIPSCs was largely eliminated in the presence of both Cd^{2+} and Ni^{2+} (Fig. 2F). These data strongly suggest that voltage-gated Ca^{2+} channels play an important role in the potentiaton of synaptic GABA release by mAChR activation in the spinal dorsal horn.

Nonselective cation channels (NSCCs) contribute to mAChR activation-induced GABA release

We have shown that activation of mAChRs has no effect on action potential-independent quantal release of GABA, suggesting that the synaptic GABA release elicited by mAChR agonists is likely due to the increased excitability of GABAergic interneurons in the spinal dorsal horn (Zhang et al., 2005). Because little is known about the signaling mechanisms underlying the stimulating effect of mAChRs on spinal GABAergic neurons, the following studies were conducted to determine the downstream signaling pathways responsible for the potentiating effect of the mAChR agonist. NSCCs appear to be involved in the stimulating effect of mAChR agonists in smooth muscles (Bolton and Zholos, 1997, Lee et al., 2003, So and Kim, 2003, Dresviannikov et al., 2006) and in cortical and hippocampal neurons (Guerineau et al., 1995, Haj-Dahmane and Andrade, 1996, 1999). Therefore, we used the NSCC blockers, 2-APB and SKF96365 (Bayguinov et al., 2001, Lievremont et al., 2005), to determine if NSCCs are involved in the stimulating effect of oxotremorine-M on synaptic GABA release to spinal dorsal horn neurons. Bath application of 10 μM 2-APB for 5 min had no significant effect on the baseline frequency of sIPSCs. The effect of oxotremorine-M on the frequency of sIPSCs was significantly attenuated by 10 μM 2-APB (n = 16, Fig. 3, A, C, and E).

Bath application of another structurally dissimilar NSCC blocker, SKF96365 (50 μM), for 5 min also significantly reduced the potentiating effect of oxotremorine-M on the frequency of sIPSCs (n = 10, Fig. 3, B-D). SKF96365 alone did not significantly change the frequency of sIPSCs. These results suggest that NSCCs are involved in the increased excitation of spinal GABAergic neurons by mAChR stimulation in the spinal dorsal horn.

KCNQ channels are not involved in synaptic GABA release induced by mAChR activation

Activation of mAChRs can inhibit KCNQ channels to increase the neuronal excitability in dissociated sympathetic neurons (Brown and Adams, 1980). KCNQ channels are also present in primary sensory neurons and seem to play an important role in the control of the excitability of nociceptive neurons (Passmore et al., 2003). We next determined the role of KCNQ in oxotremorine-M-induced excitation (depolarization) of GABAergic neurons. Bath application of 10 μM XE991, the specific KCNQ channel blocker (Passmore et al., 2003, Wladyka et al., 2007), had no significant effect on the baseline frequency of GABAergic sIPSCs. It also had no significant effect on the increase in the frequency of sIPSCs by 3 μM oxotremorine-M (n = 9, Fig. 4, A-C). These data suggest that KCNQ channels are not involved in the stimulatory effect of the mAChR agonist on GABAergic neurons in the spinal dorsal horn.

Lack of a role of adenylyl cyclase (AC) in the potentiation of synaptic GABA release by mAChR activation

Although the large contribution of M_2/M_4 subtypes to the mAChR agonist-induced increases in synaptic GABA release in the spinal cord is unexpected (Zhang et al., 2005), some evidence suggests that increased AC activity coupled to M_2/M_4 subtypes may be involved. For instance, stimulation of the M_4 subtype increases cAMP production through activation of AC II that is coupled to G_{i1} or G_{i2} proteins (Liu et al., 1999). Also, the M_2 subtype may be coupled to Gs protein to increase cAMP (Michal et al., 2007). To determine whether increased excitability

of spinal GABAergic neurons by oxotremorine-M is through increased AC activity, the specific AC inhibitor MDL12230A (Shen and Johnson, 2003), was used. Bath application of 20 μM MDL12330A alone for 10 min significantly increased the baseline frequency of sIPSCs (n = 10, Fig. 4D). However, oxotremorine-M still profoundly increased the frequency of GABAergic sIPSCs (Fig. 4D) in the presence of MDL12330A. Thus, it is less likely that the potentiation of synaptic GABA release by mAChR activation is mediated by increased AC activity in the spinal dorsal horn.

Phosphoinositide-3-kinase (PI3K) contributes to increased GABAergic input by mAChR activation

PI3K is closely involved in the stimulation of NSCCs in cell lines (Kawanabe et al., 2001, Kawanabe et al., 2003). Furthermore, PI3K is essential in the stimulating effect of the M_2 subtype on NSCCs in smooth muscle cells (Wang et al., 1999) and on voltage-gated Ca^{2+} channels in myocytes (Callaghan et al., 2004). Thus, we examined the role of PI3K in the potentiating effect of oxotremorine-M on synaptic GABA release. In this series of experiments, the spinal cord slices were pre-incubated with the specific PI3K inhibitor wortmannin (100 nM) or LY294002 (50 μM) for 1 hour because of their poor membrane permeability (Hou and Klann, 2004, Kim et al., 2007). In spinal cord slices pre-treated with 100 nM wortmannin, 3 μM oxotremorine-M significantly increased the frequency of sIPSCs in only 11 of 21 neurons (52.4%, Fig. 5, A-C). However, the increase in the frequency of sIPSCs by oxotremorine-M was significantly less than that in the absence of wortmannin (Figs. 1D and 5C). Oxotremorine-M had no significant effect on the frequency of sIPSCs in the other 10 neurons tested.

Similarly, in the spinal cord slices pre-treated with 50 μM LY294002, 3 μM oxotremorine-M significantly increased the frequency of sIPSCs in only 17 of 29 neurons (58.6%, Fig. 5D). However, the magnitude of the increase in frequency of sIPSCs by oxotremorine-M was significantly less than that in the absence of LY294002 (Figs.1D and 5D). Oxotremorine-M had no significant effect on sIPSCs in the other 12 neurons tested. These data suggest that PI3K contributes to the potentiation of the excitability of GABAergic neurons by mAChR activation in the spinal dorsal horn.

The PI3K-NSCC cascade is involved in M_2/M_4 subtype-induced synaptic GABA release

We have shown that all three mAChR subtypes (M_2, M_3, and M_4) in the spinal cord contribute to the increased GABA release induced by the mAChR agonist (Zhang et al., 2005). It would be important to determine if the PI3K-NSCC pathway is involved in the increase in synaptic GABA release by M_2/M_4 or M_3 subtypes in the spinal cord. Due to the lack of highly selective M_3 subtype antagonists, we used the siRNA approach to specifically knock down the M_3 subtype in the spinal cord to examine the role of the PI3K-NSCC cascade in M_2/M_4 subtype-mediated increase in synaptic GABA release. We first determined the neuronal uptake and distribution of the siRNA-chitosan tagged with a fluorescent dye, Alexa-555, after intrathecal injection. The siRNA fluorescence was present in the cytoplasm of neurons in the lumbar dorsal root ganglion and spinal cord within 24 hr after intrathecal injection of 5 μg of the tagged RNA encapsulated in chitosan (Fig. 6A). However, when the fluorescence-tagged siRNA was injected without chitosan, its uptake in the DRG and spinal cord was negligible.

Quantitative RT-PCR analysis revealed that intrathecal treatment with M_3 siRNA caused a large reduction in the level of M_3 mRNA in the rat spinal cord, compared with that in control siRNA-treated rats (Fig. 6B). In contrast, treatment with the M_3 siRNA had no effect on the expression levels of M_2 and M_4 mRNA in the spinal cord (Fig. 6B). We also determined the M_3 protein level in the spinal cord of M_3 siRNA- and control siRNA-treated rats (n = 6 in each group). The spinal cord membranes were labeled with a saturating concentration (2 nM) of the nonselective mAChR antagonist [^{3}H]QNB, solubilized with 1% digitonin, and then

immunoprecipitated using an M_3 subtype-selective antiserum (Chen et al., 2005). This analysis showed that the membrane protein level of the M_3 subtype was reduced by about 40% by intrathecal treatment of M_3 siRNA compared with that in control siRNA-treated rats (Fig. 6C).

After confirming the specific effect of M_3 siRNA treatment on the mRNA and protein levels of the M_3 subtype in the spinal cord, we assessed the effect of the NSCC blocker SKF96365 on oxotremorine-M-induced increases in sIPSCs in M_3 siRNA- and control siRNA-treated rats. In M_3 siRNA-treated rats, the initial effect of 3 μM oxotremorine-M on the frequency of sIPSCs was significantly reduced compared with that in control siRNA-treated rats (n = 10, Fig. 7, A-C). Furthermore, the effect of oxotremorine-M on the frequency of sIPSCs was significantly reduced in the presence of 50 μM SKF96365. The percentage by which SKF96365 inhibited the oxotremorine-M's effect on sIPSCs was not significantly different between M_3 siRNA- and control siRNA-treated rats (Fig. 7C).

To determine whether PI3K is also involved in the M_2/M_4-mediated effect on sIPSCs, the spinal cord slices from M_3 siRNA- and control siRNA-treated rats were first incubated with 100 nM wortmannin for 1 hour. In 24 of 35 (68.6%) neurons tested from M_3 siRNA-treated rats, 3 μM oxotremorine-M significantly increased the frequency of sIPSCs. However, the increase in the frequency of sIPSCs by oxotremorine-M was significantly less than that in slices not treated with wortmannin (Figs. 1D and 7D). In the remaining 11 (31.4%) neurons, oxotremorine-M had no significant effect on the frequency of sIPSCs. In 21 of 30 (70%) neurons examined from control siRNA-treated rats, 3 μM oxotremorine-M also caused a significantly smaller increase in the frequency of sIPSCs compared to the data obtained from spinal cord slices not treated with wortmannin (Figs. 1D and 7D). Oxotremorine-M had no significant effect on the frequency of sIPSCs in the other 9 neurons in control siRNA-treated rats. Therefore, although specific knockdown of the spinal M_3 subtype with siRNA significantly reduced the initial effect of oxotremorine-M on the frequency of sIPSCs, inhibition of PI3K and NSCCs still produced a similarly large attenuation of the oxotremorine-M-induced increase in sIPSCs in the spinal cord. These data suggest that the PI3K-NSCC pathway contributes to the M_2/M_4 subtype-mediated potentiation of synaptic GABA release in the spinal dorsal horn.

PI3K-NSCCs pathway is not involved in the M_3 subtype-mediated increase in synaptic GABA release

To determine whether the PI3K-NSCC cascade is involved in the M_3 subtype-mediated increase in synaptic GABA release, the effect of SKF96365 or wortmannin on the oxotremorine-M-induced increase in sIPSCs was evaluated in the presence of the specific M_2/M_4 antagonist, himbacine (Miller et al., 1992). Using spinal cord slices from mAChR subtype-knockout mice, we have shown that 2 μM himbacine specifically blocks M_2/M_4, but not the M_3, subtypes (Zhang et al., 2006a). In the following studies, we continuously perfused the spinal cord slices with 2 μM himbacine throughout the experiment. In 10 of 22 (45.5%) neurons tested, initial application of 3 μM oxotremorine-M failed to increase the frequency of sIPSCs. In the other 12 neurons, the effect of oxotremorine-M on the frequency of sIPSCs was significantly reduced compared with that in the absence of himbacine (Fig. 8, A-C). This observation is consistent with the himbacine effect observed in our previous study (Zhang et al., 2005). In these 12 neurons in which oxotremorine-M increased sIPSCs, subsequent application of 50 μM SKF96365 did not significantly alter the effect of oxotremorine-M on the frequency of sIPSCs (Fig. 8C).

Furthermore, to assess whether PI3K is involved in the M_3 subtype-mediated effect on spinal GABA release, the spinal cord slices were first incubated with 100 nM wortmannin for 1 hour. Bath application of 3 μM oxotremorine-M had no significant effect on the frequency of sIPSCs in 12 of 23 neurons (52.2%). However, oxotremorine-M still significantly increased the

frequency of sIPSCs in the remaining 11 neurons tested (Fig. 9, A-C). In these 11 neurons (47.8%), subsequent application of 2 μM himbacine had no significant effect on oxotremorine-M-induced increase in the frequency of sIPSCs (Fig. 9, A-C).

Similarly, in an additional 16 neurons, we applied 2 μM himbacine to the bath before application of oxotremorine-M. In 7 of 16 neurons, 3 μM oxotremorine-M caused a significant increase in the frequency of GABAergic sIPSCs (Fig. 9D). The magnitude of increase in the sIPSC frequency was similar to the effect of oxotremorine-M tested in the above 11 neurons. These data strongly suggest that the PI3K-NSCC pathway is not involved in the M_3 subtype-mediated potentiation of GABAergic synaptic transmission in the spinal cord.

DISCUSSION

The signaling mechanisms involved in the potentiation of spinal GABAergic synaptic transmission by mAChR activation have not been determined previously. In the present study, we found that the mAChR agonist oxotremorine-M caused a large increase in GABAergic sIPSCs, which was abolished when Ca^{2+} was removed from the extracellular solution. Blocking voltage-gated Ca^{2+} channels also profoundly reduced the potentiating effect of oxotremorine-M on sIPSCs. However, inhibition of KCNQ channels or AC activity failed to alter the oxotremorine-M's effect. Furthermore, blocking NSCCs or PI3K significantly attenuated the effect of oxotremorine-M on sIPSCs. The attenuating effect of the NSCC or PI3K blockers was still present when the M_3 subtype was specifically knocked down by intrathecal treatment of siRNA. In contrast, the effect of the NSCC or PI3K blockers on oxotremorine-M-induced sIPSCs was not observed when the M_2/M_4 subtypes were blocked with himbacine. Therefore, this study provides novel information that activation of mAChRs potentiates synaptic GABA release through Ca^{2+} influx mediated by voltage-gated Ca^{2+} channels. The PI3K-NSCC pathway is primarily responsible for the M_2/M_4 subtype-mediated excitation of GABAergic interneurons in the spinal dorsal horn.

Activation of mAChRs in the spinal cord inhibits nociceptive transmission and produces analgesia in animals and in humans (Iwamoto and Marion, 1993, Hood et al., 1997, Duttaroy et al., 2002, Chen and Pan, 2004). Stimulation of mAChRs causes a large increase in synaptic GABA release, which could attenuate glutamatergic input from primary afferents through $GABA_B$ receptors (Baba et al., 1998, Li et al., 2002, Zhang et al., 2005). Because oxotremorine-M has no effect on synaptic GABA release in the presence of the Na^+ channel blocker tetrodotoxin, oxotremorine-M-induced GABA release is caused by the increased excitability of GABAergic interneurons (Zhang et al., 2005). In this study, we determined the downstream signaling mechanisms for the potentiation of GABAergic synaptic transmission by mAChR activation in the spinal cord. We found that oxotremorine-M-induced GABAergic sIPSCs were abolished in the Ca^{2+}-free bath solution, suggesting that Ca^{2+} influx is required for increased synaptic GABA release by mAChR activation in the spinal cord. Furthermore, blocking low and high voltage-gated Ca^{2+} channels with Cd^{2+} and Ni^{2+} largely eliminated the effect of oxotremorine-M on the frequency of sIPSCs. Therefore, voltage-gated Ca^{2+} channels play an essential role in the increased intracellular Ca^{2+} levels and vesicle release from GABAergic neurons evoked by mAChR activation in the spinal cord.

The signaling pathways leading to increased excitability (depolarization) of GABAergic interneurons by mAChR activation in the spinal dorsal horn remain unclear. Stimulation of mAChRs can inhibit the "M current" or KCNQ channels in the sympathetic neurons (Brown and Adams, 1980). KCNQ channels are also present in dorsal root ganglion neurons and can control the excitability of these neurons (Passmore et al., 2003). Because these channels can be activated near the resting membrane potential, inhibition of these channels could result in the membrane depolarization. However, we found that blocking the KCNQ channels with

XE991 had no significant effect on the basal frequency of sIPSCs or on oxotremorine-M-induced increase in sIPSCs. Thus, it is unlikely that KCNQ channels are expressed on spinal GABAergic interneurons and involved in the potentiation of synaptic GABA release by mAChR activation.

We have shown that the M_2 and M_4 mAChR subtypes play a major role in the increased synaptic GABA release by the mAChR agonist in the spinal cord, because treatment with pertussis toxin to inactivate $G_{i/o}$ proteins or the selective M_2/M_4 mAChR antagonist himbacine blocks most of the effect of oxotremorine-M on GABAergic sIPSCs (Zhang et al., 2005). The functional activity of the M_4 subtype requires the presence of the M_2 mAChRs, and the M_4 subtype may form functional oligomers with the M_2 mAChRs in the spinal cord (Zhang et al., 2006b). Increased cAMP can activate protein kinase A or presynaptic hyperpolarization-activated cation channels to facilitate the release of neurotransmitters (Beaumont and Zucker, 2000, Mellor et al., 2002). It is possible that the excitatory action of M_2 and M_4 subtypes on spinal GABAergic neurons is due to their coupling to certain types of G_i proteins and AC isozymes. For example, activation of the M_4 subtype can stimulate the activity of AC isozymes II, IV, and VII (Nevo et al., 1998), and the M_4 subtype could stimulate the cAMP production through activation of AC II that is coupled to G_{i1} or G_{i2} proteins (Liu et al., 1999). However, we found that the selective AC inhibitor MDL12230A did not alter the effect of oxotremorine-M on sIPSCs. Hence, the potentiating effect of the mAChR agonist on GABA release is not through stimulating cAMP production in the spinal cord. We observed unexpectedly that MDL12230A alone increased the basal frequency of sIPSCs. It is not clear how inhibition of AC or PKA leads to increased neurotransmitter release. A similar phenomenon has been previously reported with a specific inhibitor of protein kinase A, which enhances the amplitude of excitatory junction potentials (Beaumont and Zucker, 2000).

The mAChR agonists can activate NSCCs in smooth muscle cells (Bolton and Zholos, 1997, Lee et al., 2003, So and Kim, 2003) and in dissociated neurons (Guerineau et al., 1995, Haj-Dahmane and Andrade, 1996, 1999). We found that blocking the NSCCs with two structurally distinct blockers, 2-APB or SKF96365, causes a similar inhibition of oxotremorine-M's effect on the frequency of GABAergic sIPSCs. This finding suggests that NSCCs likely mediate the stimulating effect of the mAChR agonist on the excitability of of spinal GABAergic interneurons. The *Drosophila* transient receptor potential (TRP) channels (TRPC1-7) have been recognized as molecular candidates for NSCCs. TRPC5 appears to be a candidate for NSCCs by mAChR activation in smooth muscles (Lee et al., 2003). Activation of mAChRs also can stimulate TRPC6 channels in PC12D cells (Zhang et al., 2006b). Further studies are warranted to identify the specific TRPC channels involved in potentiation of spinal GABAergic neurons by the mAChR agonist in the spinal cord.

Stimulation of PI3K can activate NSCCs in cell lines (Kawanabe et al., 2003). Activation of the M_2 subtype also enhances the voltage-gated Ca^{2+} channel current through PI3K in myocytes (Callaghan et al., 2004). Conversely, inhibition of the PI3K with LY294002 reduces mAChR-induced Ca^{2+} influx in PC12 cells (Morita et al., 2007). In this study, we found that inhibition of PI3K with two structurally dissimilar inhibitors, wortmannin and LY294002, completely blocked the effect of oxotremorine-M on the frequency of sIPSCs in 40-48% neurons. In the other neurons tested, wortmannin or LY294002 significantly inhibited the oxotremorine-M's effect. Therefore, our findings strongly suggest that PI3K-NSCC pathway is involved in the excitation of GABAergic neurons by the mAChR agonist in the spinal cord.

Although M_2 is the most abundant subtype present in the spinal cord (Hoglund and Baghdoyan, 1997, Duttaroy et al., 2002, Chen et al., 2005), the M_3 and M_4 subtypes are also involved in the potentiation of spinal GABA release (Zhang et al., 2005). Because the M_2/M_4 and M_3 subtypes are coupled to distinct G proteins, we determined whether the PI3K-NSCC pathway

is involved in M_2/M_4- or M_3-mediated increases in the excitability of spinal GABAergic neurons in the spinal cord. To study M_2/M_4-mediated effect, we used the M_3-targeting siRNA to specifically knock down this subtype because highly selective M_3 antagonists are not available. Conversely, to determine the M_3-mediated effect, we used the specific M_2/M_4 subtype-antagonist himbacine (Miller et al., 1992) to eliminate the effect produced by M_2/M_4 subtypes in the spinal cord slices. Effective delivery of siRNA to neurons in the dorsal root ganglion and spinal cord was confirmed by the neuronal uptake of fluorescence-labeled siRNA after intrathecal injection. The efficacy and specificity of the M_3 siRNA in downregulation of the M_3 subtype in the spinal cord at the mRNA and protein levels were substantiated by quantitative RT-PCR and receptor binding assays. We found that in M_3 siRNA-treated rats, the effect of oxotremorine-M on the frequency of sIPSCs was significantly attenuated by inhibition of PI3K and NSCCs with wortmannin and SKF96365, respectively. In contrast, blocking PI3K and NSCCs failed to reduce the effect of oxotremorine-M on GABAergic sIPSCs in the presence of himbacine. Therefore, these data suggest that the PI3K-NSCC signaling is most likely involved in the potentiating effect of M_2/M_4 subtypes on GABAergic interneurons in the spinal cord.

In summary, we determined the signaling mechanisms underlying the unique potentiation of the GABAergic inputs to spinal dorsal horn neurons by mAChRs. Our findings suggest that Ca^{2+} influx through voltage-gated Ca^{2+} channels is essential for the enhancement of GABAergic synaptic transmission by mAChR activation. Furthermore, the PI3K-NSCC pathway plays an important role in increased excitability of spinal GABAergic interneurons by mAChRs, and this signaling cascade is involved in the potentiating effect mediated only by M_2/M_4, but not by M_3, subtypes. This new information is important to our understanding of the signaling molecules involved in the regulation of GABAergic tone and nociceptive modulation by mAChRs in the spinal cord.

Acknowledgements

This study was supported by Grants GM64830 and NS45602 from the National Institutes of Health.

References

Baba H, Kohno T, Okamoto M, Goldstein PA, Shimoji K, Yoshimura M. Muscarinic facilitation of GABA release in substantia gelatinosa of the rat spinal dorsal horn. J Physiol 1998;508:83–93. [PubMed: 9490821]

Bao J, Li JJ, Perl ER. Differences in Ca2+ channels governing generation of miniature and evoked excitatory synaptic currents in spinal laminae I and II. J Neurosci 1998;18:8740–8750. [PubMed: 9786981]

Bayguinov O, Hagen B, Sanders KM. Muscarinic stimulation increases basal Ca(2+) and inhibits spontaneous Ca(2+) transients in murine colonic myocytes. Am J Physiol Cell Physiol 2001;280:C689–700. [PubMed: 11171588]

Beaumont V, Zucker RS. Enhancement of synaptic transmission by cyclic AMP modulation of presynaptic Ih channels. Nat Neurosci 2000;3:133–141. [PubMed: 10649568]

Bolton TB, Zholos AV. Activation of M2 muscarinic receptors in guinea-pig ileum opens cationic channels modulated by M3 muscarinic receptors. Life Sci 1997;60:1121–1128. [PubMed: 9121356]

Brown DA, Adams PR. Muscarinic suppression of a novel voltage-sensitive K+ current in a vertebrate neurone. Nature 1980;283:673–676. [PubMed: 6965523]

Callaghan B, Koh SD, Keef KD. Muscarinic M2 receptor stimulation of Cav1.2b requires phosphatidylinositol 3-kinase, protein kinase C, and c-Src. Circ Res 2004;94:626–633. [PubMed: 14739158]

Caulfield MP, Birdsall NJ. International Union of Pharmacology. XVII. Classification of muscarinic acetylcholine receptors. Pharmacol Rev 1998;50:279–290. [PubMed: 9647869]

Caulfield MP, Jones S, Vallis Y, Buckley NJ, Kim GD, Milligan G, Brown DA. Muscarinic M-current inhibition via G alpha q/11 and alpha-adrenoceptor inhibition of Ca2+ current via G alpha o in rat sympathetic neurones. J Physiol 1994;477:415–422. [PubMed: 7932231]

Chen SR, Pan HL. Activation of muscarinic receptors inhibits spinal dorsal horn projection neurons: role of GABAB receptors. Neuroscience 2004;125:141–148. [PubMed: 15051153]

Chen SR, Wess J, Pan HL. Functional activity of the M2 and M4 receptor subtypes in the spinal cord studied with muscarinic acetylcholine receptor knockout mice. J Pharmacol Exp Ther 2005;313:765–770. [PubMed: 15665136]

Dresviannikov AV, Bolton TB, Zholos AV. Muscarinic receptor-activated cationic channels in murine ileal myocytes. Br J Pharmacol 2006;149:179–187. [PubMed: 16894345]

Duttaroy A, Gomeza J, Gan JW, Siddiqui N, Basile AS, Harman WD, Smith PL, Felder CC, Levey AI, Wess J. Evaluation of muscarinic agonist-induced analgesia in muscarinic acetylcholine receptor knockout mice. Mol Pharmacol 2002;62:1084–1093. [PubMed: 12391271]

Evellin S, Nolte J, Tysack K, vom Dorp F, Thiel M, Weernink PA, Jakobs KH, Webb EJ, Lomasney JW, Schmidt M. Stimulation of phospholipase C-epsilon by the M3 muscarinic acetylcholine receptor mediated by cyclic AMP and the GTPase Rap2B. J Biol Chem 2002;277:16805–16813. [PubMed: 11877431]

Guerineau NC, Bossu JL, Gahwiler BH, Gerber U. Activation of a nonselective cationic conductance by metabotropic glutamatergic and muscarinic agonists in CA3 pyramidal neurons of the rat hippocampus. J Neurosci 1995;15:4395–4407. [PubMed: 7790916]

Haj-Dahmane S, Andrade R. Muscarinic activation of a voltage-dependent cation nonselective current in rat association cortex. J Neurosci 1996;16:3848–3861. [PubMed: 8656279]

Haj-Dahmane S, Andrade R. Muscarinic receptors regulate two different calcium-dependent non-selective cation currents in rat prefrontal cortex. Eur J Neurosci 1999;11:1973–1980. [PubMed: 10336666]

Hoglund AU, Baghdoyan HA. M2, M3 and M4, but not M1, muscarinic receptor subtypes are present in rat spinal cord. J Pharmacol Exp Ther 1997;281:470–477. [PubMed: 9103533]

Hood DD, Mallak KA, James RL, Tuttle R, Eisenach JC. Enhancement of analgesia from systemic opioid in humans by spinal cholinesterase inhibition. J Pharmacol Exp Ther 1997;282:86–92. [PubMed: 9223543]

Hou L, Klann E. Activation of the phosphoinositide 3-kinase-Akt-mammalian target of rapamycin signaling pathway is required for metabotropic glutamate receptor-dependent long-term depression. J Neurosci 2004;24:6352–6361. [PubMed: 15254091]

Howard KA, Rahbek UL, Liu X, Damgaard CK, Glud SZ, Andersen MO, Hovgaard MB, Schmitz A, Nyengaard JR, Besenbacher F, Kjems J. RNA interference in vitro and in vivo using a novel chitosan/siRNA nanoparticle system. Mol Ther 2006;14:476–484. [PubMed: 16829204]

Iwamoto ET, Marion L. Characterization of the antinociception produced by intrathecally administered muscarinic agonists in rats. J Pharmacol Exp Ther 1993;266:329–338. [PubMed: 8101218]

Katas H, Alpar HO. Development and characterisation of chitosan nanoparticles for siRNA delivery. J Control Release 2006;115:216–225. [PubMed: 16959358]

Kawanabe Y, Hashimoto N, Masaki T. Effects of nonselective cation channels and PI3K on endothelin-1-induced PYK2 tyrosine phosphorylation in C6 glioma cells. Am J Physiol Cell Physiol 2003;285:C539–545. [PubMed: 12900387]

Kawanabe Y, Hashimoto N, Masaki T, Miwa S. Ca(2+) influx through nonselective cation channels plays an essential role in noradrenaline-induced arachidonic acid release in Chinese hamster ovary cells expressing alpha(1A)-, alpha(1B)-, or alpha(1D)-adrenergic receptors. J Pharmacol Exp Ther 2001;299:901–907. [PubMed: 11714874]

Kim SE, Lee WJ, Choi KY. The PI3 kinase-Akt pathway mediates Wnt3a-induced proliferation. Cell Signal 2007;19:511–518. [PubMed: 17011750]

Lee YM, Kim BJ, Kim HJ, Yang DK, Zhu MH, Lee KP, So I, Kim KW. TRPC5 as a candidate for the nonselective cation channel activated by muscarinic stimulation in murine stomach. Am J Physiol Gastrointest Liver Physiol 2003;284:G604–616. [PubMed: 12631560]

Li DP, Chen SR, Pan YZ, Levey AI, Pan HL. Role of presynaptic muscarinic and GABA(B) receptors in spinal glutamate release and cholinergic analgesia in rats. J Physiol 2002;543:807–818. [PubMed: 12231640]

Lievremont JP, Bird GS, Putney JW Jr. Mechanism of inhibition of TRPC cation channels by 2-aminoethoxydiphenylborane. Mol Pharmacol 2005;68:758–762. [PubMed: 15933213]

Liu X, Howard KA, Dong M, Andersen MO, Rahbek UL, Johnsen MG, Hansen OC, Besenbacher F, Kjems J. The influence of polymeric properties on chitosan/siRNA nanoparticle formulation and gene silencing. Biomaterials 2007;28:1280–1288. [PubMed: 17126901]

Liu YF, Ghahremani MH, Rasenick MM, Jakobs KH, Albert PR. Stimulation of cAMP synthesis by Gi-coupled receptors upon ablation of distinct Galphai protein expression. Gi subtype specificity of the 5-HT1A receptor. J Biol Chem 1999;274:16444–16450. [PubMed: 10347206]

May LG, Johnson S, Krebs S, Newman A, Aronstam RS. Involvement of protein kinase C and protein kinase A in the muscarinic receptor signalling pathways mediating phospholipase C activation, arachidonic acid release and calcium mobilisation. Cell Signal 1999;11:179–187. [PubMed: 10353692]

Mellor J, Nicoll RA, Schmitz D. Mediation of hippocampal mossy fiber long-term potentiation by presynaptic Ih channels. Science 2002;295:143–147. [PubMed: 11778053]

Michal P, El-Fakahany EE, Dolezal V. Muscarinic M2 receptors directly activate Gq/11 and Gs G-proteins. J Pharmacol Exp Ther 2007;320:607–614. [PubMed: 17065363]

Miller JH, Aagaard PJ, Gibson VA, McKinney M. Binding and functional selectivity of himbacine for cloned and neuronal muscarinic receptors. J Pharmacol Exp Ther 1992;263:663–667. [PubMed: 1331410]

Morita M, Yoshizaki K, Nakane A, Kudo Y. Inhibitory effect of the phosphoinositide 3-kinase inhibitor LY294002 on muscarinic acetylcholine receptor-induced calcium entry in PC12h cells. J Pharmacol Sci 2007;105:258–263. [PubMed: 17965536]

Nevo I, Avidor-Reiss T, Levy R, Bayewitch M, Heldman E, Vogel Z. Regulation of adenylyl cyclase isozymes on acute and chronic activation of inhibitory receptors. Mol Pharmacol 1998;54:419–426. [PubMed: 9687584]

Passmore GM, Selyanko AA, Mistry M, Al-Qatari M, Marsh SJ, Matthews EA, Dickenson AH, Brown TA, Burbidge SA, Main M, Brown DA. KCNQ/M currents in sensory neurons: significance for pain therapy. J Neurosci 2003;23:7227–7236. [PubMed: 12904483]

Scatton B, Dubois A, Javoy-Agid F, Camus A. Autoradiographic localization of muscarinic cholinergic receptors at various segmental levels of the human spinal cord. Neurosci Lett 1984;49:239–245. [PubMed: 6493605]

Shen KZ, Johnson SW. Group II metabotropic glutamate receptor modulation of excitatory transmission in rat subthalamic nucleus. J Physiol 2003;553:489–496. [PubMed: 14500768]

So I, Kim KW. Nonselective cation channels activated by the stimulation of muscarinic receptors in mammalian gastric smooth muscle. J Smooth Muscle Res 2003;39:231–247. [PubMed: 15048016]

Villiger JW, Faull RL. Muscarinic cholinergic receptors in the human spinal cord: differential localization of [3H]pirenzepine and [3H]quinuclidinylbenzilate binding sites. Brain Res 1985;345:196–199. [PubMed: 3840715]

Wang YX, Dhulipala PD, Li L, Benovic JL, Kotlikoff MI. Coupling of M2 muscarinic receptors to membrane ion channels via phosphoinositide 3-kinase gamma and atypical protein kinase C. J Biol Chem 1999;274:13859–13864. [PubMed: 10318793]

Wess J. Novel insights into muscarinic acetylcholine receptor function using gene targeting technology. Trends Pharmacol Sci 2003;24:414–420. [PubMed: 12915051]

Wladyka CL, Feng B, Glazebrook PA, Schild JH, Kunze DL. The KCNQ/M-current modulates arterial baroreceptor function at the sensory terminal in rats. J Physiol 2007;586:795–802. [PubMed: 18048450]

Wu ZZ, Chen SR, Pan HL. Differential sensitivity of N- and P/Q-type Ca2+ channel currents to a mu opioid in isolectin B4-positive and -negative dorsal root ganglion neurons. J Pharmacol Exp Ther 2004;311:939–947. [PubMed: 15280436]

Yamamura HI, Wamsley JK, Deshmukh P, Roeske WR. Differential light microscopic autoradiographic localization of muscarinic cholinergic receptors in the brainstem and spinal cord of the rat using [3H] pirenzepine. Eur J Pharmacol 1983;91:147–149. [PubMed: 6688587]

Yung KK, Lo YL. Immunocytochemical localization of muscarinic m2 receptor in the rat spinal cord. Neurosci Lett 1997;229:81–84. [PubMed: 9223596]

Zhang HM, Chen SR, Matsui M, Gautam D, Wess J, Pan HL. Opposing functions of spinal M2, M3, and M4 receptor subtypes in regulation of GABAergic inputs to dorsal horn neurons revealed by muscarinic receptor knockout mice. Mol Pharmacol 2006a;69:1048–1055. [PubMed: 16365281]

Zhang HM, Li DP, Chen SR, Pan HL. M2, M3, and M4 receptor subtypes contribute to muscarinic potentiation of GABAergic inputs to spinal dorsal horn neurons. J Pharmacol Exp Ther 2005;313:697–704. [PubMed: 15640398]

Zhang L, Guo F, Kim JY, Saffen D. Muscarinic acetylcholine receptors activate TRPC6 channels in PC12D cells via Ca2+ store-independent mechanisms. J Biochem 2006b;139:459–470. [PubMed: 16567411]

Zhuo M, Gebhart GF. Tonic cholinergic inhibition of spinal mechanical transmission. Pain 1991;46:211–222. [PubMed: 1661000]

List of abbreviations

AC
: adenylyl cyclase

GABA
: γ-aminobutyric acid

GDP-β-S
: guanosine 5’-*O*-(2-thiodiphosphate)

sIPSCs
: spontaneous inhibitory postsynaptic currents

mAChRs
: muscarinic acetylcholine receptors

NSCCs
: nonselective cation channels

PI3K
: phosphoinositide-3-kinase

siRNA
: small interfering RNA

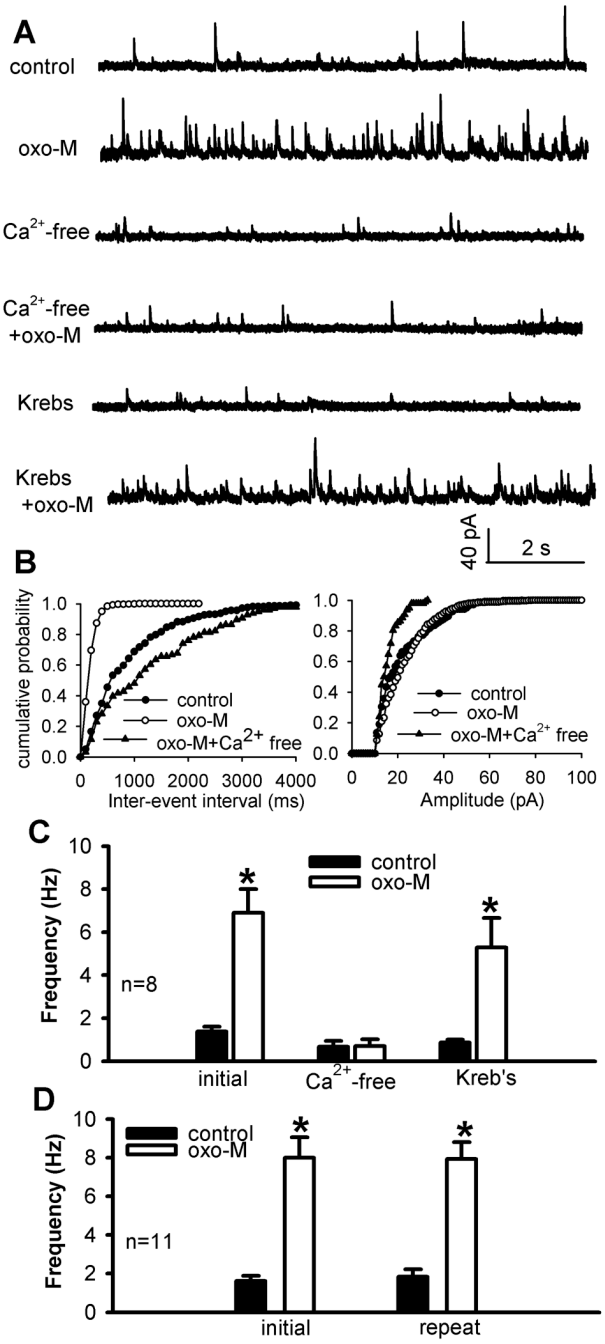

Fig. 1.

Effect of oxotremorine-M on GABAergic sIPSCs of lamina II neurons was abolished in Ca^{2+}-free solution. A, Representative traces show GABAergic sIPSCs of one lamina II neuron during control, application of 3 μM oxotremorine-M (oxo-M) in either Ca^{2+}-free or Krebs solution. B, Cumulative distribution plots of the inter-event interval and amplitude of sIPSCs of the same neuron in A during control and application of oxotremorine-M in either Ca^{2+}-free or Krebs solution. C, Summary data show the effect of oxotremorine-M on sIPSCs was abolished in Ca^{2+}-free solution but recovered in Krebs solution (n = 8). D, Group data show that repeated application of 3 μM oxotremorine-M had a reproducible effect on the frequency

of sIPSCs (n = 11). Data are presented as means ± S.E.M. *, $P < 0.05$ compared with the pre-drug control.

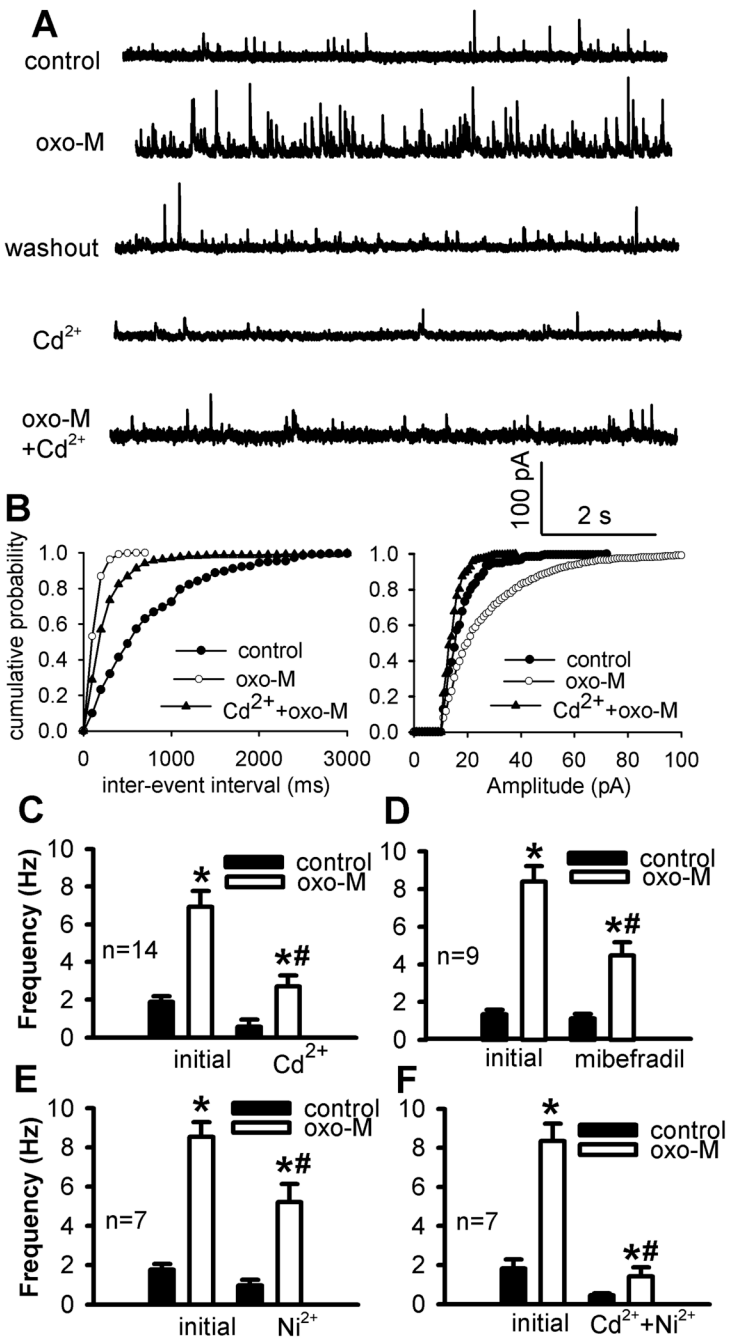

Fig. 2.

Effect of blocking high and low voltage-gated Ca^{2+} channels on oxotremorine-M-induced increases in GABAergic sIPSCs. A, Original traces show sIPSCs of one lamina II neuron during control, application of 3 μM oxotremorine-M, 100 μM Cd^{2+} alone, and Cd^{2+} plus oxotremorine-M (oxo-M). B, Cumulative distribution plots of the inter-event interval and amplitude of sIPSCs of the same neuron in A during control and application of oxotremorine-M with and without Cd^{2+}. C, Summary data show that 100 μM Cd^{2+} significantly blocked the effect of oxotremorine-M on the frequency of sIPSCs. D-F, Group data show the effects of 100 μM mibefradil, 100 μM Ni^{2+}, and Cd^{2+}plus Ni^{2+}on 3 μM oxotremorine-M-induced increases

in the frequency of sIPSCs. Data are presented as means ± S.E.M. *, $P < 0.05$ compared with the pre-drug control. #, $P < 0.05$ compared with the initial effect of oxotremorine-M.

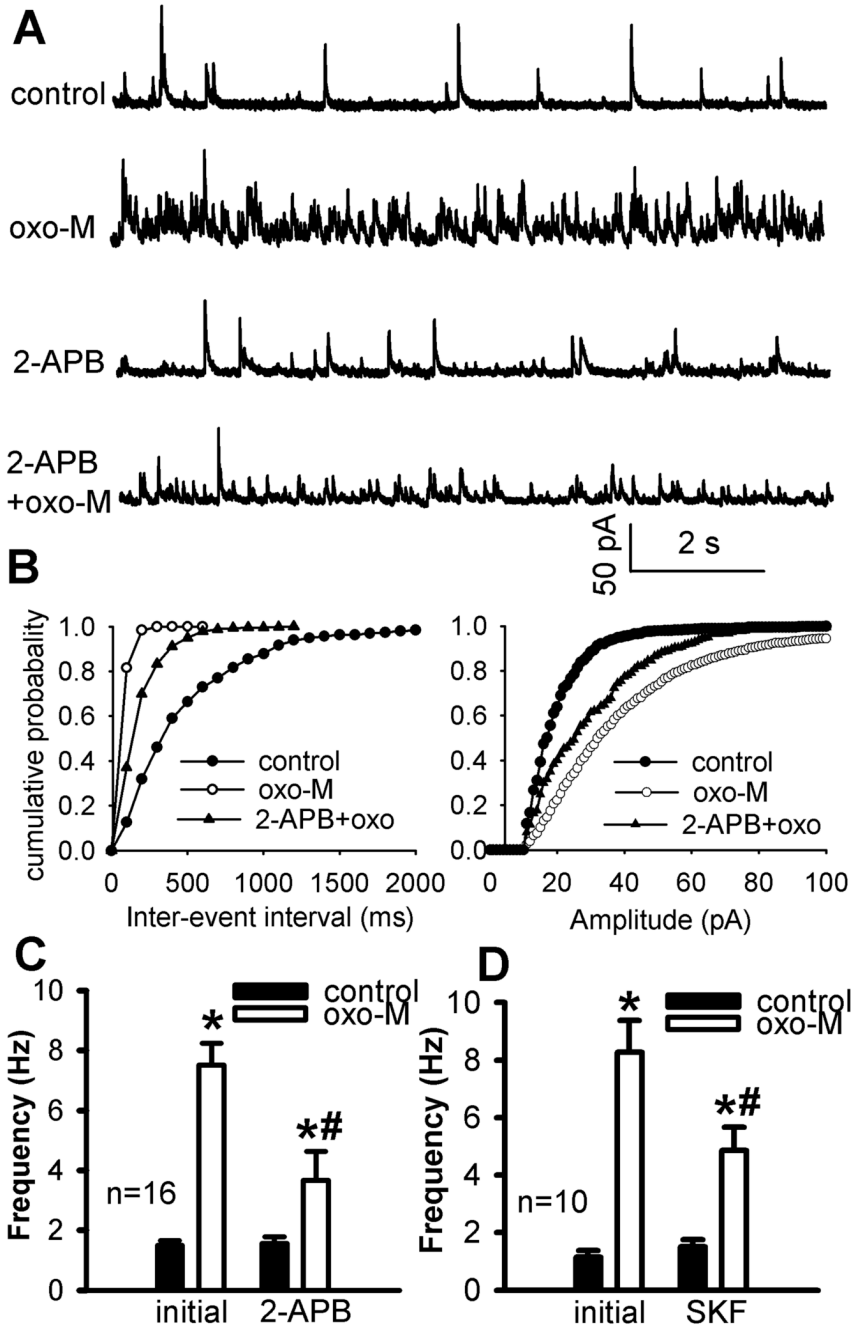

Fig. 3.

Effect of blocking NSCCs with 2-APB or SKF96365 on oxotremorine-M-induced increases in GABAergic sIPSCs of lamina II neurons. A and B, Representative traces of sIPSCs during control and application of 3 μM oxotremorine-M (oxo-M) with 10 μM 2-APB or 50 μM SKF96365 (SKF) in 2 separate lamina II neurons. C and D, Cumulative distribution plots of the inter-event interval and amplitude of sIPSCs of the same neuron in A and B during control and application of oxotremorine-M with and without 2-APB or SKF96365. E and F, Summary data show the effect of oxotremorine-M on the frequency of GABAergic sIPSCs of lamina II neurons with and without 10 μM 2-APB or 50 μM SKF96365. Data presented as means ±

S.E.M. *, $P < 0.05$ compared with re-drug controls. #, $P < 0.05$ compared with the initial effect of oxotremorine-M.

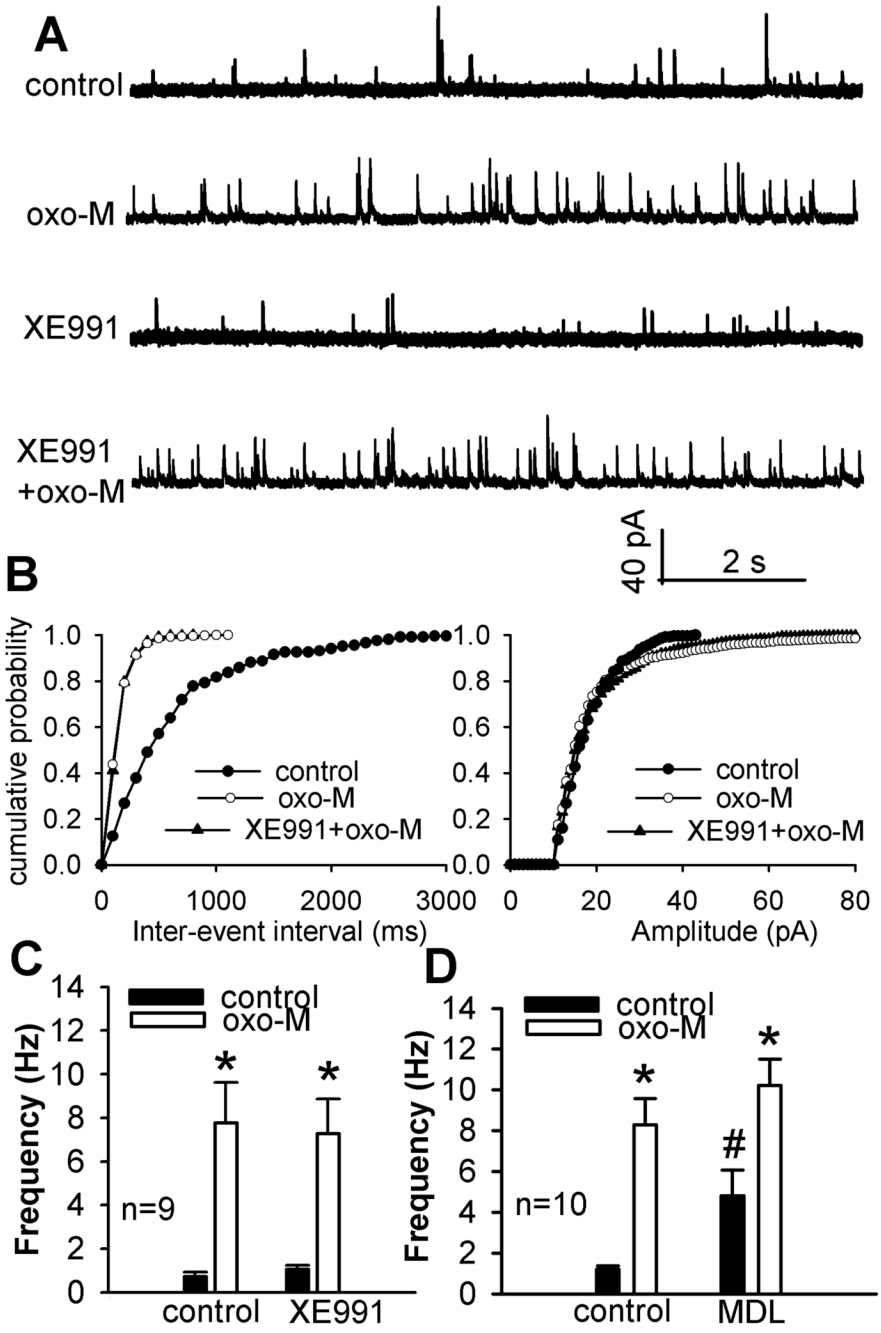

Fig. 4.

Lack of effect of KCNQ channel blocker XE991 or the adenylate cyclase inhibitor MDL12230A on oxotremorine-M-induced increases in sIPSCs of lamina II neurons. A, Raw traces of GABAergic sIPSCs of one lamina II neuron during control, application of 3 μM oxotremorine-M (oxo-M), 10 μM XE991 alone, and XE991 plus oxotremorine-M. B, Cumulative distribution plots of the inter-event interval and amplitude of sIPSCs of the same neuron in A during control and application of oxotremorine-M with and without XE991. C, Summary data show that 10 μM XE991 had no significant effect on oxotremorine-M-induced increase in the frequency of sIPSCs of 9 lamina II neurons. D, Summary data show that 20 μM MDL12230A (MDL) had no effect on oxotremorine-M-induced increases in the frequency

of sIPSCs of another 10 neurons. Data are presented as means ± S.E.M. *, $P < 0.05$ compared with the pre-drug control. #, $P < 0.05$ compared with the initial baseline control.

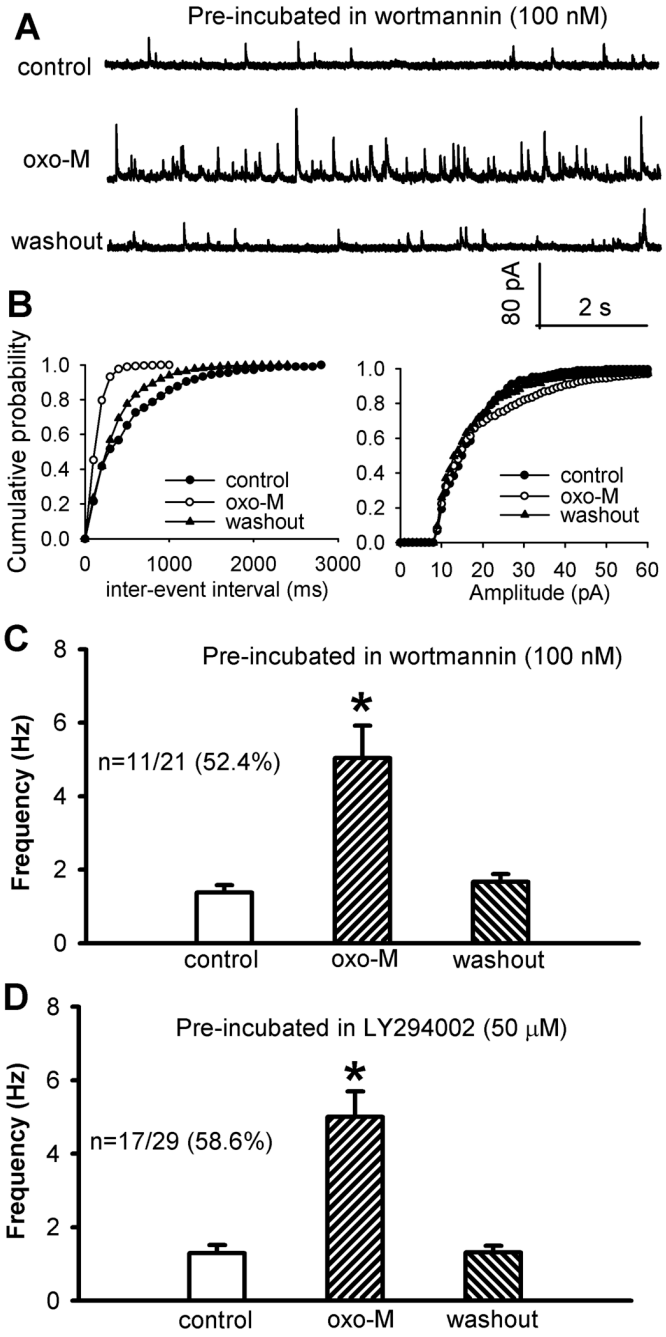

Fig. 5.

Effect of pre-incubation of the spinal slices with the PI3K inhibitor wortmannin or LY294002 on oxotremorine-M-induced increase in GABAergic sIPSCs of lamina II neurons. A, Representative traces of sIPSCs during control and application of 3 μM oxotremorine-M (oxo-M) in one lamina II neuron after wortmannin (100 nM) treatment. B, Cumulative distribution plots of the inter-event interval and amplitude of sIPSCs of the same neuron in A. C and D, Summary data show the effect of oxotremorine-M on the frequency of GABAergic sIPSCs of lamina II neurons pretreated with 100 nM wortmannin or 50 μM LY294002. Data are presented as means ± S.E.M. *, $P < 0.05$ compared with the respective controls.

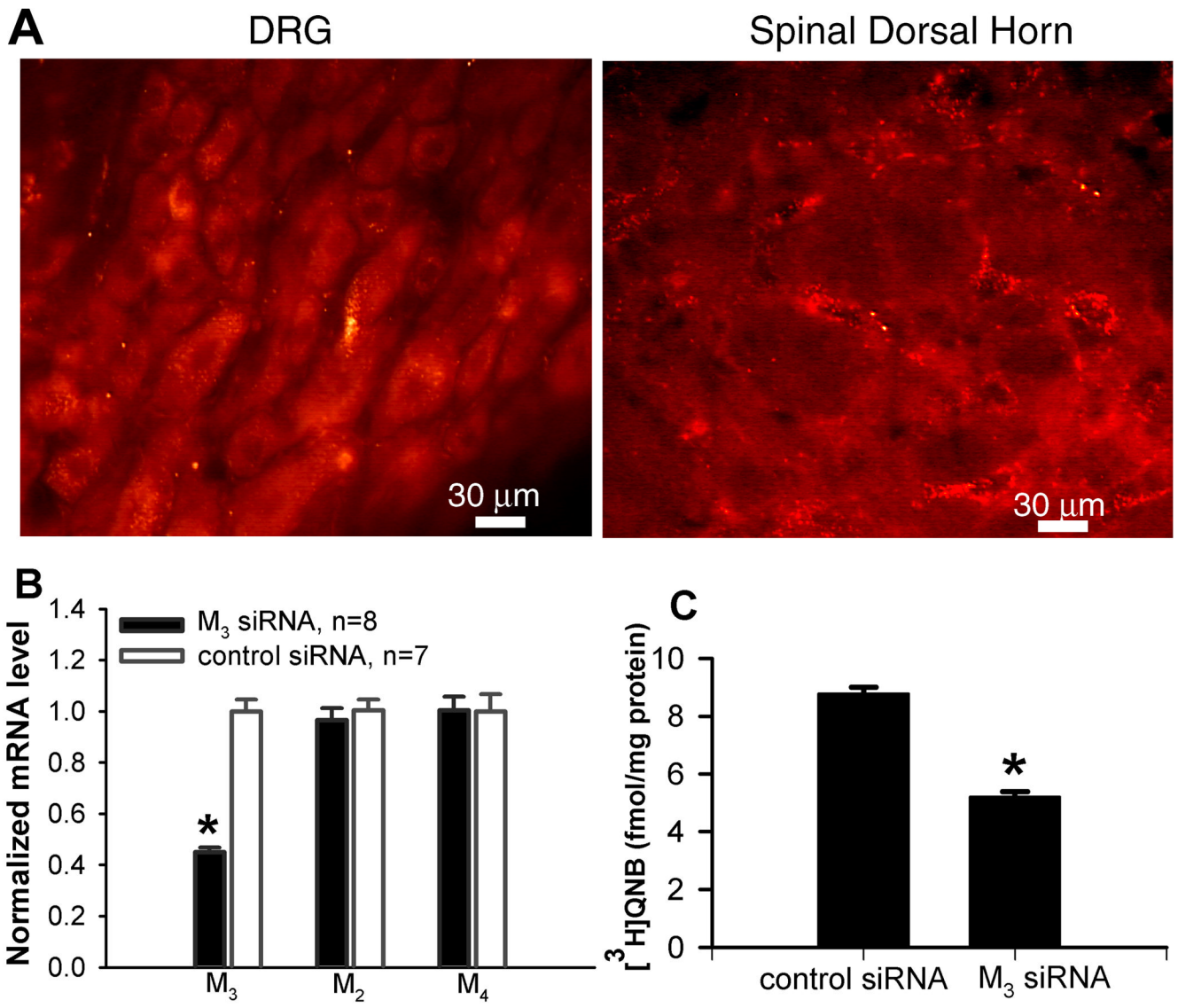

Fig. 6.

Effect of intrathecal treatment of M_3 siRNA on the levels of M_3 mRNA and protein in the spinal cord. A, Micrographs showing the neuronal uptake of the siRNA-chitosan tagged with Alexa-555 (red fluorescent particles in the cytoplasm) in the lumbar dorsal root ganglion (DRG) and spinal dorsal horn 24 hr after intrathecal injection in one rat. B, Effect of intrathecal treatment of M_3 siRNA and control siRNA on the expression level of M_2, M_3, and M_4 mRNA in the spinal cord determined by real-time RT-PCR. C, Quantification of the M_3 membrane protein level in the spinal cord of M_3 siRNA- and control siRNA-treated rats. Membrane proteins were incubated with [^{3}H]QNB. [^{3}H]QNB-labeled mAChRs were then solubilized and immunoprecipitated using an M_3 subtype-selective antiserum. Data are presented as means ± S.E.M. *, $P < 0.05$ compared with the value in the control siRNA group.

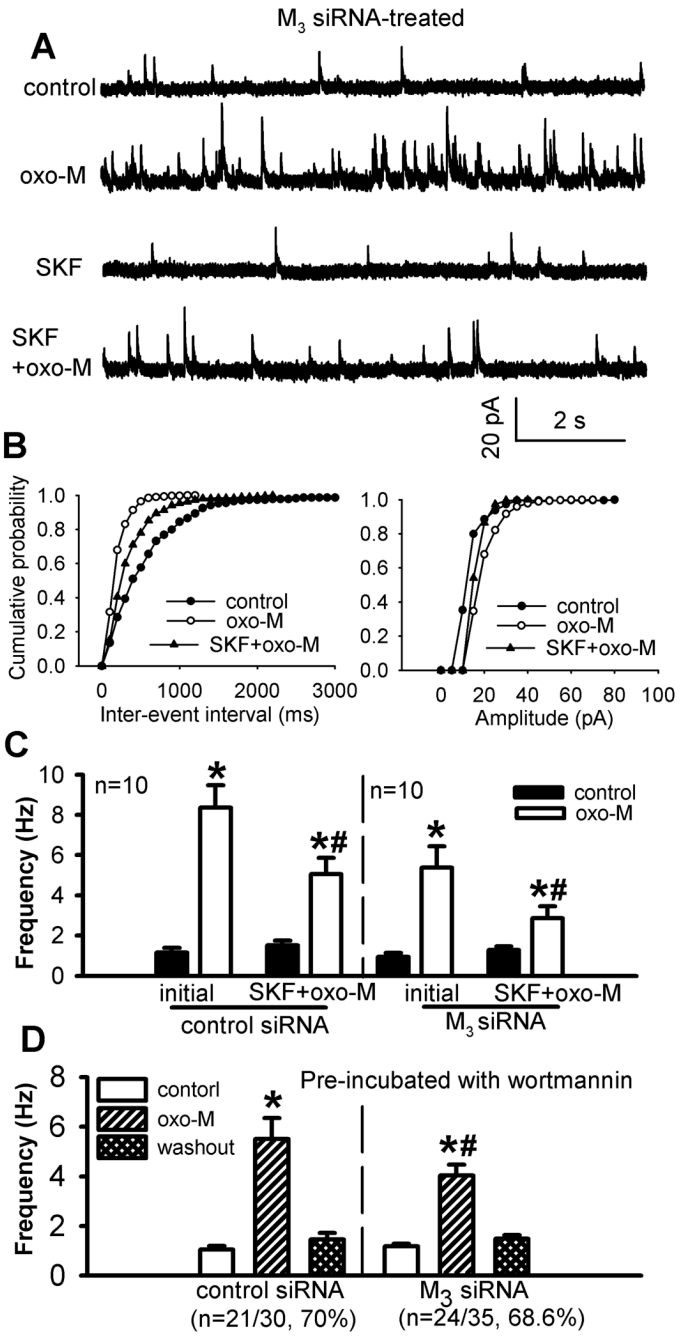

Fig. 7.

Effect of SKF96365 or wortmannin on oxotremorine-M-induced increase in GABAergic sIPSCs of lamina II neurons from M_3 siRNA-treated rats. A, Representative traces of sIPSCs of one lamina II neuron during control and application of 3 μM oxotremorine-M (oxo-M) with and without 50 μM SKF96365. B, Cumulative distribution plots of the inter-event interval and amplitude of sIPSCs of the same neuron in A. C, Summary data show the effect of 50 μM SKF96365 on oxotremorine-M-induced increase in the frequency of GABAergic sIPSCs of lamina II neurons in M_3 siRNA- and control siRNA-treated rats. D. Summary data show the effect of oxotremorine-M on the frequency of GABAergic sIPSCs of lamina II neurons pre-treated with 100 nM wortmannin in M_3 siRNA- and control siRNA-treated rats. Data are

presented as means ± S.E.M. *, $P < 0.05$ compared with the pre-drug control. #, $P < 0.05$ compared with the initial effect of oxotremorine-M.

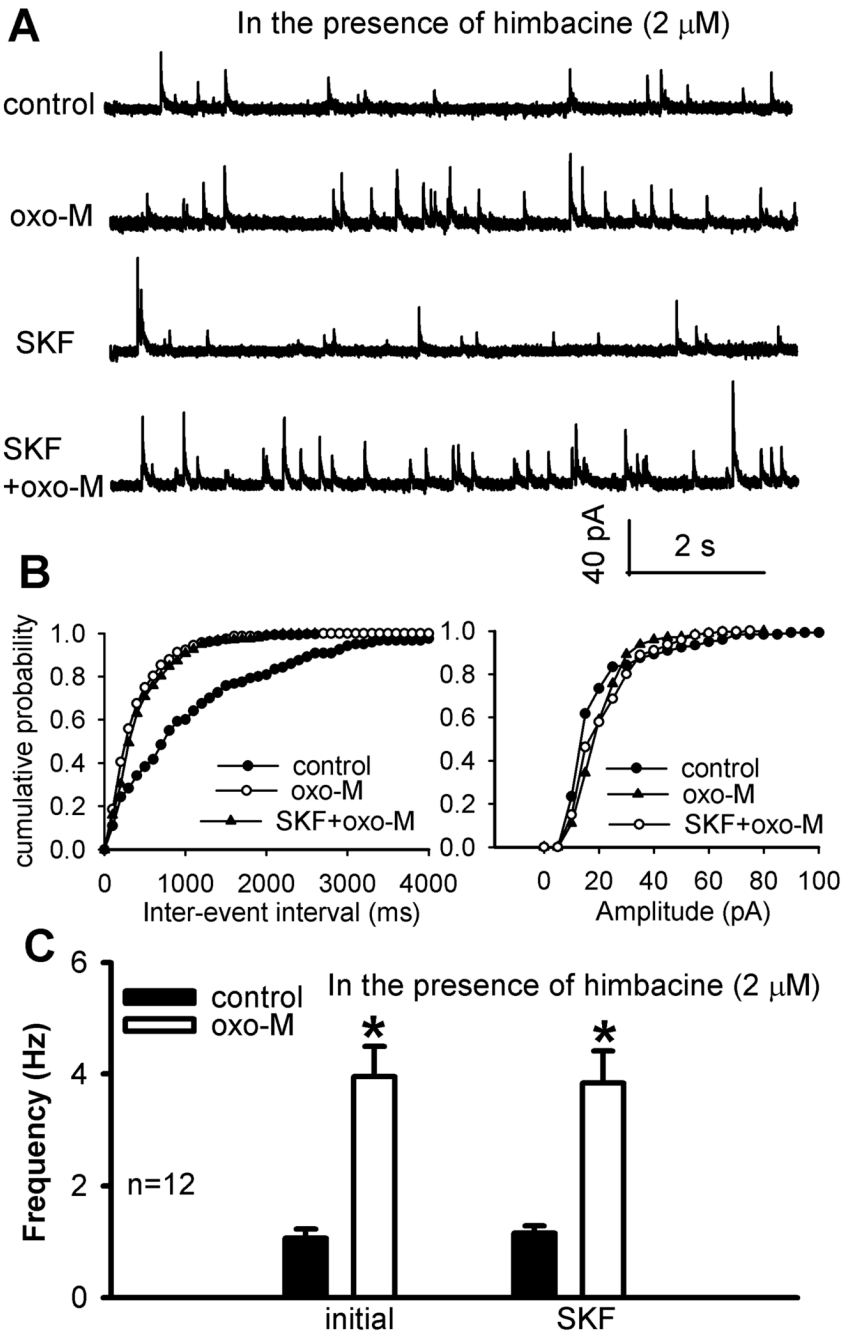

Fig. 8.

Effect of SKF96365 on oxotremorine-M-induced increase in GABAergic sIPSCs of lamina II neurons in the presence of himbacine. A, Representative traces of sIPSCs of one lamina II neuron during control and application of 3 μM oxotremorine-M (oxo-M) with and without 50 μM SKF96365. Himbacine (2 μM) was perfused throughout the experiment. B, Cumulative distribution plots of the inter-event interval and amplitude of sIPSCs of the same neuron in A during control and application of oxotremorine-M with and without SKF96365. C, Summary data show the lack of effect of SKF96365 on oxotremorine-M-induced increase in the frequency of GABAergic sIPSCs of lamina II neurons in the presence of 2 μM himbacine. Data are presented as means ± S.E.M. *, $P < 0.05$ compared with the pre-drug control.

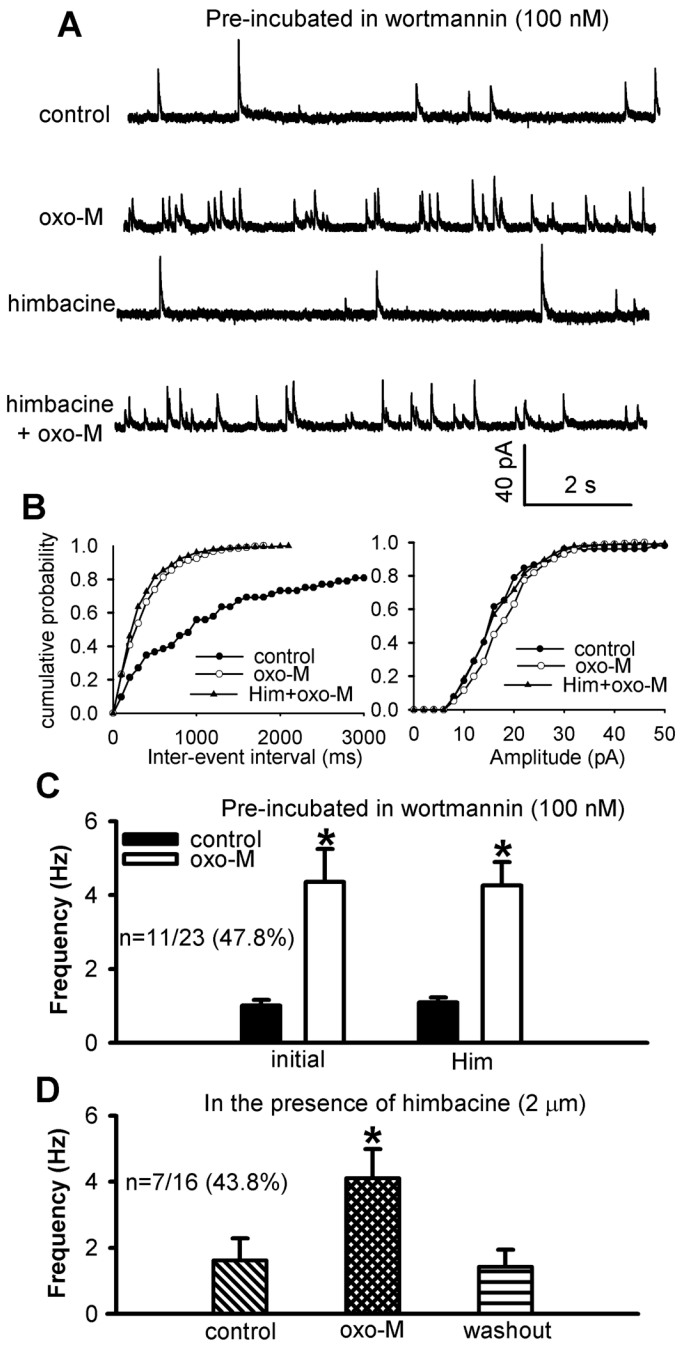

Fig. 9.

Effect of wortmannin on oxotremorine-M-induced increases in GABAergic sIPSCs of lamina II neurons in the presence of himbacine. A, Representative traces of sIPSCs during control and application of 3 μM oxotremorine-M (oxo-M) with and without 2 μM himbacine in one lamina II neuron pretreated with 100 nM wortmannin. B, Cumulative distribution plots of the inter-event interval and amplitude of sIPSCs of the same neuron in A. C, Summary data show the lack of an effect of 2 μM himbacine on oxotremorine-M-induced increase in the frequency of sIPSCs of lamina II neurons pre-treated with wortmannin. D, Group data show the reduced effect of 3 μM oxotremorine-M on the frequency of sIPSCs of lamina II neurons pre-treated

with both 2 μM himbacine and 100 nM wortmannin. Data are presented as means ± S.E.M. *, $P < 0.05$ compared with the pre-drug control.

Table 1

List of primers used for real-time RT-PCR

Gene Amplicon (bp)	Primer sequence
M_2	Forward: 5’-TCCCGGGCAAGCAAGAGTAGAATAAAGA-3’
142	Reverse: 5’-CCAGGCCGCCATCACCACCAG-3’
M_3	Forward: 5’-ACCACGGCTACTCTACCTCTGTCCTTCA- 3’
131	Reverse: 5’-AGCGTCTGGGCGGCCTTCTTCTC-3’
M_4	Forward: 5’-GCCCCTGGGTGCCGTGGTCTGTGA-3’
137	Reverse: 5’-GGCGGGCGGGATAGGTGAGGGGTTTG-3’
β-actin	Forward: 5’-TGAACCCTAAGGCCAACCGTGAAAAGAT-3’
111	Reverse: 5’-GACCAGAGGCATACAGGGACAACACAGC-3’